High-pressure ignition plasma torch for aerospace testing facilities

D I Yusupov, Yu M Kulikov, M Kh Gadzhiev, A S Tyuftyaev and E E Son

Joint Institute for High Temperatures of the Russian Academy of Sciences, Izhorskaya 13 Bldg 2, Moscow 125412, Russia

E-mail: spt_yusupov@mail.ru

Abstract. The present paper discusses the issues of implementation of high-pressure ignition plasma torch in terms of discharge phenomena in compressed gases, dense nitrogen plasma properties and stable arcing power requirements. Contact ignition has been tested in a pressure range $p = 1$–25 bar and has proved to be a reliable solution for pilot arc burning.

1. Introduction

Combustion gases can be used for primary flow preheating to extend the operating range of aerodynamic tunnel plants aimed for aerospace testing. Ignition devices which in particular are powerful spark plugs have to operate in severe environment characterized by very high breakdown voltage. Considerable fuel mixture flow rates (up to 200 kg/s) require excessive spark current that leads to accelerated deterioration of electrodes.

A high-pressure plasma torch poses a reasonable alternative to spark plug ignition of combustive mixture in wind tunnel facilities.

Low-temperature plasma generators with an axial gas flow are usually designed [1] to have a cylindrical channel with a constant cross-section. A negative voltage–current characteristic, low thermal efficiency and unstable operation are the most serious shortcomings of such plasma torches, causing redundant power consumption and shorten life cycle.

As a framework for present studies, we employed high-efficient vortex-stabilized direct current plasma torch completed with divergent duct [2, 3] that provides stable electrical arc operation conditions. Nitrogen was used as the well-studied plasma-supporting gas providing a sufficient electrode lifetime.

This paper deals with adapting of proven in use atmospheric plasma torch to an operation at pressures up to $p = 25$ bar and flow rates up to $G = 0.01$ kg/s. The following sections are aimed to highlight the problems of reliable electrode gap breakdown, as well as maintaining of stable arcing and to provide the estimates of plasma torch required power basing on the calculated thermal plasma properties. The last section is focused on testing of arc ignition system of the device.

2. Electrical breakdown phenomena in compressed gases

Breakdown properties of a high-pressure gas being a working fluid for the plasma generator possess a number of remarkable features particularly related to a significant deviation from

Paschen law. This law relates breakdown voltage U_b to a gas pressure and an electrode gap via the formula

$$U_b = \frac{a(pd)}{\ln(pd) + b}. \tag{1}$$

Data analysis [4] of the breakdown voltage U_b at higher $pd > 6000$ Pa m shows that U_b begins to flatten out despite the pressure increase. Moreover, there is a large variation of the breakdown voltage (± 15 kV) along with the increase of a mean value when the electrode gap size decreases. A smaller gap provides a shorter diffusion time for a seed electron to leave an anode-cathode path. Paschen law violation in compressed gas may be associated with the flash of electron emission. Such an ejection from a cathode surface in case of nitrogen can contain up to 10^6 electrons [5].

The breakdown voltage U_b in a uniform electrical field at a gas pressure up to several bar is independent [6] of the breakdowns number produced. Conversely, at higher pressures, when electrical field strength is about 10 MV/m the breakdown voltage increases with the number of breakdowns asymptotically reaching a constant value. This phenomenon called spark-conditioning [7] particularly for nitrogen yields 2.5-fold growth of U_b compared to the first breakdown voltage after 100 sparks.

The required number of sparks for the conditioning and the final breakdown voltage increases with electrodes area enlargement and the electrical field applied. Hundreds or even thousands of sparks may be sometimes required to provide properly conditioned electrode surface [8]. Furthermore, the breakdown field in compressed gases depends strongly on the presence of dust particles, the electrode material and surface processing conditions. Thus, the use of high voltage breakdown for pilot arc ignition causes the same problems as in spark-plug operation and seems to be impractical.

The characteristic time of the processes involved in the electrical breakdown falls in the range 10^{-6}–10^{-8} s, so that applying an alternating electric field of comparable frequency significantly reduces [9] the breakdown voltage, as this field accelerates charged particles in anode-cathode gap. The transfer of alternating electric field energy to electrons is accompanied by losses due to electron-atomic and electron-molecular collisions. On the other hand, a collisional ionization is complemented by the diffusion of positive ions. The intensity of these processes is determined by the sort of gas, its density, an electric field strength and frequency and by the geometry of the electrodes.

The following section presents estimates of the transport properties of the nitrogen plasma at high pressures and an optimal frequency of electromagnetic field applied.

3. Nitrogen plasma properties calculation for high-pressure plasma torch

When the ionization degree α is small the drift and diffusion of charged particles are determined by their collisions with neutral atoms and molecules. If α exceeds 10^{-4}–10^{-2} the collisions of charged particles with each other step forward. Both the ionization degree for ions of different multiplicity and species concentrations are determined by a chain of reactions including a dissociation and a detachment of all valence electrons [10].

A collision rate ν in gas is defined by

$$\nu = nv'\sigma^{(1)}, \tag{2}$$

where n, v', $\sigma^{(1)}$ denote particle concentration, incident velocity and transport cross-section area respectively. As for the velocity v' of the impinging particle one can use the most probable velocity of thermal motion arising from Maxwellian distribution

$$v' = \sqrt{\frac{8k_BT}{\pi m'}}. \tag{3}$$

Total cross section in case of Coulomb potential is determined by Rutherford formula

$$\sigma^{(1)} = \left(\frac{2Ze^2}{m'v^2}\right)\ln\Lambda = \left(\frac{2Ze^2}{3k_BT}\right)\ln\Lambda, \tag{4}$$

where Z denotes ion multiplicity, e—the electron charge, m'—effective (reduced) mass, k_B—Bolzmann constant, T—kinetic temperature of particles, $\ln\Lambda$—Coulomb logarithm. Then the expression for impingement frequency reduces to

$$\nu = \frac{4\sqrt{8}Z^2e^4n}{9\sqrt{\pi}(k_BT)^{3/2}(m')^{1/2}}\ln\Lambda. \tag{5}$$

In particular for electron-electron collisions we obtain

$$\nu_{\mathrm{ee}} = \frac{16e^4n_e}{9\sqrt{\pi}(k_BT)^{3/2}(m')^{1/2}}\ln\Lambda, \tag{6}$$

and similarly for collisions with ions of different multiplicity

$$\nu_{\mathrm{ee}} = \frac{8\sqrt{2}Z^2e^4n_{I^{+z}}}{9\sqrt{\pi}(k_BT)^{3/2}(m_e)^{1/2}}\ln\Lambda. \tag{7}$$

Electron total collision frequency equals to

$$\nu_C = \nu_{\mathrm{ee}} + \sum_{Z=1}^{6}\nu_{eI^{+z}} = \left(\sqrt{2}n_e + n_{I^{+1}} + 4n_{I^{+2}} + 9n_{I^{+3}} + 16n_{I^{+4}} + 25n_{I^{+5}} + 36n_{I^{+6}}\right) \times \frac{8\sqrt{2}}{9\sqrt{\pi}}\frac{e^4\ln\Lambda}{(4\pi\epsilon_0)^2(k_BT)^{3/2}(m_e)^{1/2}}. \tag{8}$$

We calculate Coulomb logarithm in accordance with

$$\ln\Lambda = \ln\left(2/\theta_{\min}\right), \tag{9}$$

where minimal scattering angle

$$\theta_{\min} = \frac{2Ze^2}{4\pi\epsilon_0 mv^2\rho_{\max}}, \tag{10}$$

and $\rho_{\max}$ denotes an impact parameter. For classical plasma conditions one can set $\rho_{\max}$ to be equal to Debye radius r_D and $\left\langle mv^2/2\right\rangle = 3/2k_BT$. For the following we introduce plasma perfectness parameter

$$\Gamma = \frac{Ze^2}{4\pi\epsilon_0 r_D k_BT}. \tag{11}$$

That bring us to

$$\ln\Lambda = \ln(2/\theta_{\min}) = \ln\left(\frac{mv^2r_D4\pi\epsilon_0}{Ze^2}\right) = \ln\left(\frac{3k_BTr_D\,4\pi\epsilon_0}{Ze^2}\right) = \ln\left(3/\Gamma\right). \tag{12}$$

One can easily relate Γ to Debye radius r_D and average charge of scattering center $\overline{Z}$:

$$\frac{1}{r_D^2} = \sum_k \frac{n_ke^2Z_k^2}{\epsilon_0T_kk_B}, \quad \overline{Z} = \frac{\sum_{Z=1}^{6}Zn_{I^{+z}}}{\sum_{Z=1}^{6}n_{I^{+z}}}, \tag{13}$$

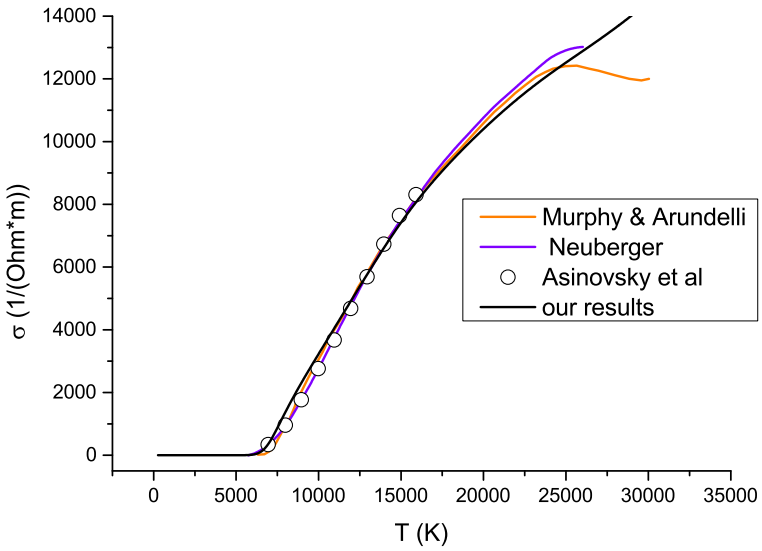

Figure 1. Nitrogen plasma conductivity at the pressure $p = 1$ bar provided by various papers.

wherein k denotes summation over all particle species. Along with charged particles collision rate ν_C, total collisional frequency ν_e also includes the contribution from electron-atomic

$$\nu_{\mathrm{eA}} = n_A \sqrt{\frac{8k_BT}{\pi m'}} \sigma_{\mathrm{eA}}^{(1)} = n_N \sqrt{\frac{8k_BT}{\pi m_e}} \sigma_{e-N}^{(1)}, \quad \sigma_{e-N}^{(1)} \approx 2 \times 10^{-20} \text{ m}^2 \tag{14}$$

and electron-molecular interactions

$$\nu_{\mathrm{eM}} = n_M \sqrt{\frac{8k_BT}{\pi m'}} \sigma_e^{(1)} M = 2n_{N_2} \sqrt{\frac{8k_BT}{\pi m_e}} \sigma_{e-N}^{(1)}, \tag{15}$$

that finally yields $\nu_e = \nu_C + \nu_{\mathrm{eA}} + \nu_{\mathrm{eM}}$, where factor 2 in (15) arises from collision center doubling in N_2 molecule. We calculate plasma conductivity $\hat{\sigma}$ via the formula

$$\hat{\sigma} = \frac{n_e e^2}{m_e \nu_e}. \tag{16}$$

The contribution of ν_C was taken into account only if $r_D < 10^{-4}$ m.

The proposed method of conductivity calculation proved to be consistent compared to the results of other authors [11–13] presented in figure 1. The pure nitrogen conductivity graphs depicted in figure 2 appear to have a reference temperature $T^* \approx 12000$ K, so that high pressure gas conductivity starts exceeding the low-pressure one. Indeed, if $T < T^*$ the ionization process shifts to a higher temperature range with increasing pressure, whereas at $T > T^*$ the concentration of free electrons (figure 3) becomes proportional to the pressure, because the ionization is already complete.

One can also provide the following estimates of electrical field frequency confirmed by other studies [14] resonant to the rate of electron-molecular collisions

$$\nu_{\mathrm{eM}} = nv'\sigma^{(1)} = 2\frac{p}{k_BT}\sqrt{\frac{8k_BT}{\pi m_e}}\sigma^{(1)} = \frac{4\sqrt{2}p\sigma^{(1)}}{\sqrt{\pi k_BTm_e}} \approx 1.04 \times 10^{11} \text{ Hz}. \tag{17}$$

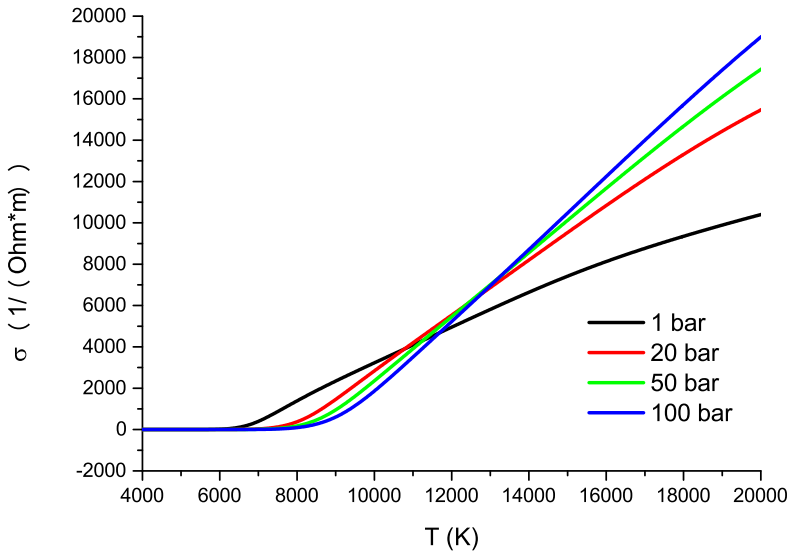

Figure 2. Nitrogen plasma conductivity at different pressures in the temperature range up to $T = 20000$ K.

The effective collision frequency ν_{En} corresponding to energy loss equals to

$$\nu_{\mathrm{En}} = \nu_{\mathrm{eM}} \frac{m_e}{M_N} \approx 0.4 \times 10^7 \text{ Hz}. \tag{18}$$

Since electron accelerates in one direction for half period, then $f = 2\nu_{\mathrm{En}} = 8 \times 10^6$ Hz at atmospheric pressure. Similarly at pressure $p = 25$ bar this frequency equals to $f = 2 \times 10^8$ Hz.

Positive ions or at least a portion of them located at the interelectrode spacing and influenced by homogeneous but high-frequency field do not have enough time to reach the cathode for a half-cycle of the applied voltage. The result is a positive ion space charge oscillating between the electrodes.

The successive electronic avalanches are the main source of space charge growth eventually leading to a breakdown. By virtue of such an accumulation effect the RF breakdown occurs at lower voltages compared to a constant field breakdown or to 50 Hz AC. The critical frequency of electric filed f_c that generates positive space charge is determined by [14]

$$f_c = \frac{K^+ E_0}{\pi d}, \tag{19}$$

wherein d, K^+, E_0 denote gap length, ion mobility and field amplitude correspondingly.

According to (17), (18) one should use a tunable RF-power source to provide optimal breakdown characteristics. The disadvantages of this solution include the streamwise spread of dangerous electromagnetic radiation in the installation interior and issues of electromagnetic compatibility with other measuring equipment. Such obstacles, as well as the complexity of the high-voltage insulation of live parts force to abandon physically subtle solutions in favor of robust contact ignition (striking).

4. High-pressure plasma torch power evaluation

Grounding the results of [10] one can estimate the required plasma torch power calculating the specific heat temperature dependence at various pressures. These curves shown in figure 4

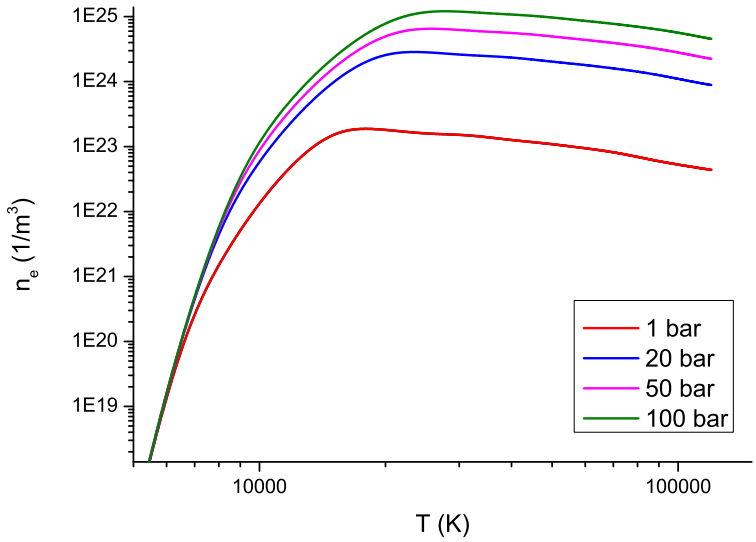

Figure 3. Concentration of electrons as a function of temperature (T = 5000–120000 K) at different pressures in logarithmic scales.

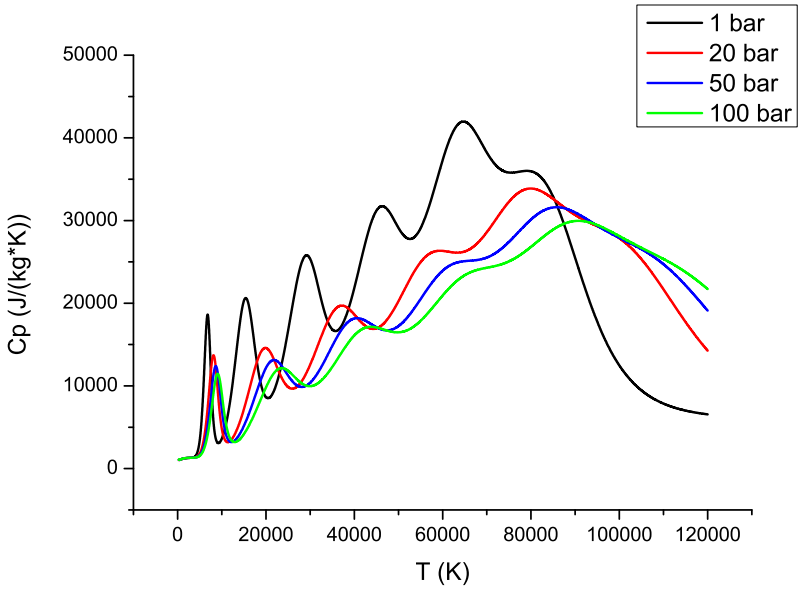

Figure 4. Nitrogen specific heat at different pressures in the wide temperature range up to T = 120000 K.

possess several peaks which local maxima diminish, as well as creep to higher temperatures with pressure increasing.

Integrating nitrogen specific heat curves over temperature range yields specific enthalpy functions $h = h(T)$. Provided initial $T_1 \approx 300$ K and final temperatures $T_2 \approx 6000$ K and gas flow rate $G \approx 0.01$ kg/s one can calculate the required power of facility P_+ at pressure

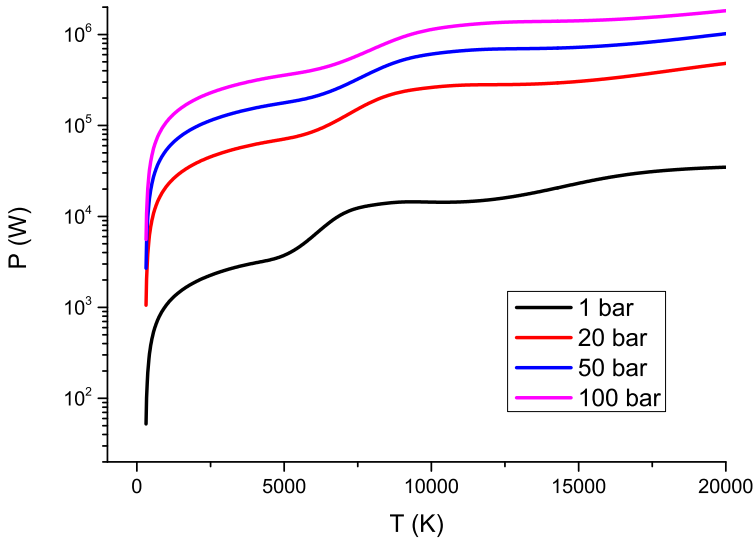

Figure 5. Arc power as a function of the bulk temperature on the assumption of a sound speed gas outflow through the critical portion. It should be noted that the maximum power at $T = 6000$ K approximately 2.5-fold higher than W_+ as a transonic outflow rate exceeds the target value ($G = 0.01$ kg/s) in 2.5 times.

$p = 20$ bar $P_+ \approx \Delta h\, G \approx 8 \times 10^2$ kW. Assuming the sound speed gas effusion in a critical portion of the nozzle (diameter $d = 9$ mm) we can estimate the power demand with respect to gas acceleration as $P \approx (\Delta h + 1/2a^2)\rho a S$ wherein P, ρ, a, S denote a power, a density, a sound speed and a cross section square. Figure 5 shows the required arc power supply P as a function of exhaust gas average temperature at various static pressures. It is worth noting the maximum power at $T = 6000$ K is approximately 2.5 times higher compared to P_+ as the flow rate at transonic mode is either 2.5-fold higher than the design flow rate ($G = 0.01$ kg/s).

5. Plasma torch ignition testing

As a standard method of pilot arc ignition in atmospheric plasma torch we used high-voltage spark igniter, however, increasing operating pressure required to implement the contact ignition supplied with the dc power source V-TTP-2K-460-UKhL4 (the output voltage is $U_i = 460$ V, the maximum output current is $I = 2000$ A).

Figure 6 shows a schematic diagram of an uncooled prototype of plasma torch under testing. A gas enters an insulated body of plasma torch, passes through tangential swirl channels speeding up in the narrow area between cathode 1 and the nozzle 2. Then the swirled gas moves through a divergent nozzle towards the anode 4.

The ignition occurs when an auxiliary rod-shaped tungsten electrode 3 is detached from cathode surface 1. After that a pilot arc with a current up to $I = 200$ A burns for a short time (figure 7) while the ionized gas is blown streamwise through the anode and then proceeds to the main arc ($I = 175$ A). The first voltage maximum corresponds to the source idle run value. Closing tungsten rod to the cathode drops voltage nearly to zero and increases the current. Succeeding rod retraction ignites the arc and coincides with voltage increase and further voltage stabilization together with current.

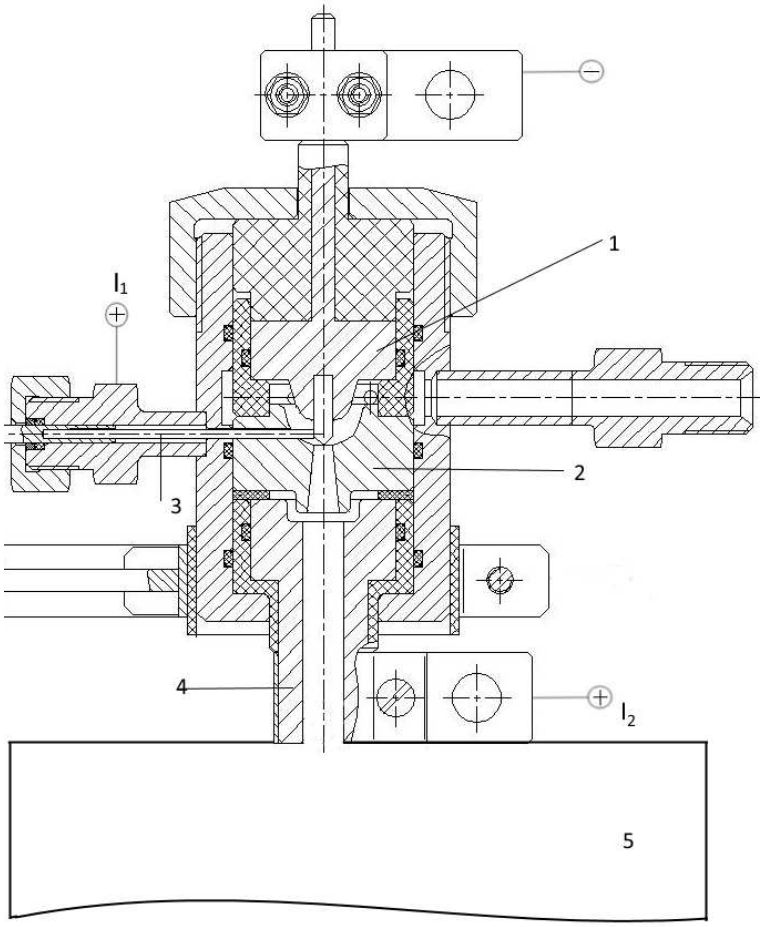

Figure 6. High-pressure plasma torch scheme: 1—copper cathode with tungsten rod, 2—nozzle, 3—tungsten rod-shaped ignition electrode, 4—anode, 5—high-pressure chamber; current-voltage measuring points: I1—pilot arc, I2—main arc.

Table 1. Electrical characteristics of high-pressure plasma torch at various pressures and gas flow rates.

p, bar	G, kg/s	I, A	U, V
1	0.002	150	120
5	0.0035	150	160
10	0.0057	150	200
15	0.007	150	200
20	0.0076	175	210
25	0.008	175	210

We carried out a series of short tests (up to 5 s) that proved the implemented contact ignition system to be robust. The major electrical characteristics of plasma torch after ignition at various pressures and gas flow rates are listed in table 1 showing that maximum voltage and current values increase with the growth of pressure.

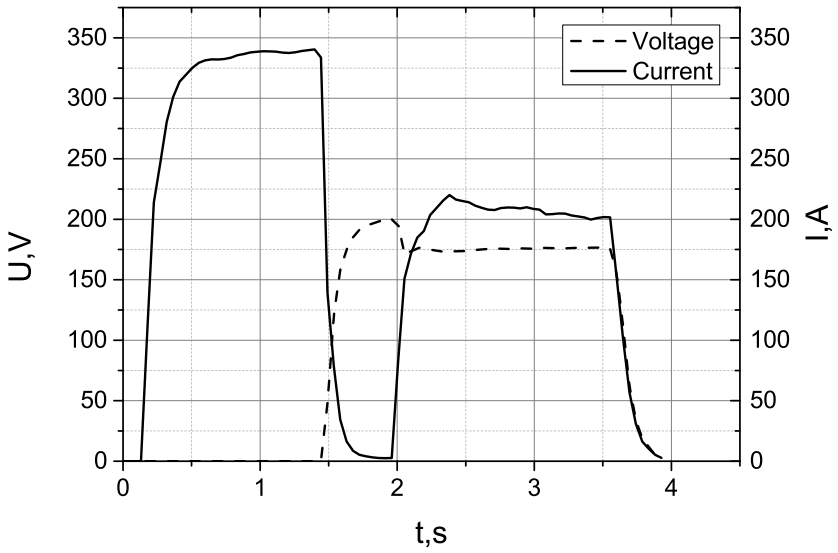

Figure 7. Voltage–time and current–time curves at $p = 20$ bar, and gas flow rate $G = 7$ g/s.

6. Conclusion

The high-pressure plasma torch developing requires overcoming a number of obstacles associated with a gas-tightness requirements and the stable arc operation. Paschen law violation in dense gases, a large variation of breakdown voltage, electrodes conditioning force to abandon the standard spark breakdown and to choose a simple and reliable striking technique. According to our results the high-pressure plasma conductivity reduces significantly compared to the atmospheric values (if $T \lesssim 12000$ K), and grows for higher temperatures. Enthalpy curves analysis shows that power requirements gradually increase proportionally to pressure. When testing we achieved a stable plasma torch ignition in the pressure range $p = 1$–25 bar, that indicates the reliability of current striking technique implementation. The obtained experimental data and approved engineering solutions will be used as in further design of cooled long-life plasma torch.

Acknowledgments

The authors wish to thank their colleague Vladislav A Panov for the fruitful discussions.

The work was supported by the Russian Science Foundation (project No. 14-50-00124).

References

[1] Zhukov M F and Zasypkin I M 2007 *Thermal Plasma Torches: Design, Characteristics, Applications* (Cambridge International Science Publishing)
[2] Isakaev E K, Sinkevich O A, Tyuftyaev A S and Chinnov V F 2010 *High Temp.* **48** 97–125
[3] Gadzhiev M K, Isakaev E K, Tyuftyaev A S and Yusupov D I 2016 *Tech. Phys. Lett.* **42** 79–81
[4] Carey W J, Wiebe A J, Nord R D and Altgilbers L L 2011 *Pulsed Power Conference (PPC), 2011 IEEE* pp 741–744
[5] Cookson A H and Ward B W 1965 *Electron. Lett.* **1** 83–84
[6] Cookson A H 1970 *Proc. Inst. Electr. Eng.* **117** 269–280
[7] Goldspink G F, Cookson A H and Lewis T J 1966 *IEE Colloquium on Gaseous Insulation* pp 1–5
[8] Howell A H 1939 *Electr. Eng. (Am. Inst. Electr. Eng.)* **58** 193–206
[9] Abou-Seada M S 1984 *IEEE Trans. Ind. Appl.* **IA-20** 1627–1630

[10] Gadzhiev M K, Kulikov Y M, Panov V A, Son E E and Tyuftyaev A S 2016 *High Temp.* **54** 38–45
[11] Murphy A B and Arundelli C J *Plasma Chem. Plasma Process.* **14** 451–490
[12] Neuberger A W 1975 *AIAA J.* **13** 3–4
[13] Asinovsky E I, Kirillin A V, Pakhomov E P and Shabashov V I 1971 *Proc. IEEE* **59** 592–601
[14] Nasser E 1971 *Fundamentals of Gaseous Ionization and Plasma Electronics* Wiley Series in Plasma Physics (John Wiley & Sons Canada, Limited)